

# Clustering of Fluorine-Substituted Alcohols as a Factor Responsible for Their Marked Effects on Proteins and Peptides

Dong-Pyo Hong,<sup>†</sup> Masaru Hoshino,<sup>‡</sup> Ryoichi Kuboi,<sup>†</sup> and Yuji Goto<sup>\*,‡</sup>

Contribution from the Department of Chemical Science Engineering, Graduate School of Engineering Science, Osaka University, 1-3 Machikaneyama, Toyonaka, Osaka 560-8531, Japan, and the Institute for Protein Research, Osaka University, 3-2 Yamadaoka, Suita, Osaka 565-0871, Japan

Received March 15, 1999

**Abstract:** Among various alcohols, those substituted with fluorine, such as 2,2,2-trifluoroethanol (TFE) or 3,3,3,3',3',3'-hexafluoro-2-propanol (HFIP), have a marked potential to induce the formation of  $\alpha$ -helical structures in peptides and to denature the native structures of proteins. However, the mechanism by which these alcohols exert their effects is unknown. Melittin, a bee venom peptide, is unfolded in the absence of alcohol, but is transformed to an  $\alpha$ -helical structure upon addition of alcohols. On the other hand, addition of alcohols to  $\beta$ -lactoglobulin, a predominantly  $\beta$ -sheet protein, denatures the molecule and transforms it to an  $\alpha$ -helical structure. We examined the role of several factors in these alcohol-induced transitions, i.e., relative dielectric constant, strength of hydrogen bond estimated by the pH titration of salicylic acid, and clustering of alcohol molecules measured by solution X-ray scattering. Although relative dielectric constant and hydrogen bond strength were confirmed to be important, they did not explain the marked effects of TFE and HFIP. X-ray scattering detected clusters of TFE or HFIP molecules in alcohol/water mixtures with a maximum at around 30% (v/v) of each alcohol. When the conformational transitions induced by TFE and HFIP were plotted against the extent of cluster formation by the corresponding alcohol/water mixtures, the TFE and HFIP-induced transition curves agreed with each other for both melittin and  $\beta$ -lactoglobulin. This suggests that clustering of alcohol molecules is an important factor that enhances the effects of alcohols on proteins and peptides.

## Introduction

The effects of alcohols on proteins and peptides have been studied extensively over the last few decades.<sup>1</sup> 2,2,2-Trifluoroethanol (TFE)<sup>2</sup> has often been used for such studies because of its marked ability to induce helical structures in peptides and to denature the native structures of proteins.<sup>3</sup> Recently, 3,3,3,3',3',3'-hexafluoro-2-propanol (HFIP) has become widely employed as an alcohol with a much stronger effect than TFE.<sup>4–7</sup> However, it is still unclear why, among the various alcohols, TFE and HFIP are so effective.

\* To whom correspondence should be addressed. Fax: +81-6-6879-8614. Email: ygoto@protein.osaka-u.ac.jp.

<sup>†</sup> Graduate School of Engineering Science.

<sup>‡</sup> Institute for Protein Research.

(1) (a) Schrier, E. E.; Ingwall, R. T.; Scheraga, H. A. *J. Phys. Chem.* **1965**, *69*, 298–303. (b) Brandts, J. F.; Hunt, L. *J. Am. Chem. Soc.* **1967**, *89*, 4826–4838. (c) Bianchi, E.; Rampone, R.; Tealdi, A.; Ciferri, A. *J. Biol. Chem.* **1970**, *245*, 3341–3345. (d) Parodi, R. M.; Bianchi, E.; Ciferri, A. *J. Biol. Chem.* **1973**, *248*, 4047–4051. (e) Velicelebi, G.; Sturtevant, J. M. *Biochemistry* **1979**, *18*, 1180–1186. (f) Fink, A. L.; Painter, B. *Biochemistry* **1987**, *26*, 1665–1671.

(2) Abbreviations: CD, circular dichroism; cmc, critical micelle concentration; HFIP, 3,3,3,3',3',3'-hexafluoro-2-propanol; TFE, 2,2,2-trifluoroethanol;  $\Delta G_t$ , Gibbs free energy change of transfer;  $\epsilon_r$ , relative dielectric constant; SDS, sodium dodecyl sulfate.

(3) (a) Nelson, J. W.; Kallenbach, N. R. *Proteins Struct. Funct. Genet.* **1986**, *1*, 211–217. (b) Segawa, S.; Fukuno, T.; Fujiwara, K.; Noda, Y. *Biopolymers* **1991**, *31*, 497–509. (c) Buck, M.; Radford, S. E.; Dobson, C. M. *Biochemistry* **1993**, *32*, 669–678. (d) Jasanoff, A.; Fersht, A. R. *Biochemistry* **1994**, *33*, 2129–2135. (e) Buck, M.; Schwalbe, H.; Dobson, C. M. *J. Mol. Biol.* **1996**, *257*, 669–683. (f) Buck, M. *Q. Rev. Biophys.* **1998**, *31*, 297–355.

(4) (a) Zhang, H.; Kaneko, K.; Nguyen, J. T.; Livshits, T. L.; Baldwin, M. A.; Cohen, F. E.; James, T. L.; Prusiner, S. B. *J. Mol. Biol.* **1995**, *250*, 514–526. (b) Barrow, C. J.; Yasuda, A.; Kenny, P. T.; Zagorski, M. G. *J. Mol. Biol.* **1992**, *225*, 1075–1093. (c) Wood, S. J.; Maleeff, B.; Hart, T.; Wetzel, R. *J. Mol. Biol.* **1996**, *256*, 870–877.

(5) Hirota, N.; Mizuno, K.; Goto, Y. *Protein Sci.* **1997**, *6*, 416–421.

(6) Hirota, N.; Mizuno, K.; Goto, Y. *J. Mol. Biol.* **1998**, *275*, 365–378.

(7) Hirota-Nakaoka, N.; Goto, Y. *Bioorg. Med. Chem.* **1999**, *7*, 67–73.

The effects of alcohols on proteins are considered to arise from the low polarity of the solvent.<sup>8–11</sup> This low polarity weakens the hydrophobic interactions that stabilize the compact native structure of proteins, but simultaneously strengthens electrostatic interactions such as hydrogen bonds, thus stabilizing secondary structures, particularly the  $\alpha$ -helix. Uversky et al.<sup>12</sup> showed that there is a high correlation between the extent of conformational transition of  $\beta$ -lactoglobulin and the relative dielectric constant ( $\epsilon_r$ ) of several organic solvents such as methanol, ethanol, 2-propanol, and dimethylformamide.

Alternatively, the effects of low polarity can be interpreted in terms of the transfer free energy ( $\Delta G_t$ ) of protein groups from water to alcohol solvent.<sup>11</sup> The water to alcohol  $\Delta G_t$  values of hydrophobic groups are negative, and those of polar groups such as amide groups are positive. Therefore, in alcohol solvents, hydrophobic groups tend to be exposed while polar amide groups tend to be buried, resulting in the formation of an “open helix” or “open helical coil”, i.e., solvent-exposed helical structures.<sup>10,11,13</sup> Liu and Bolen<sup>11</sup> indicated that the sum of  $\Delta G_t$  for each group can explain the alcohol-induced denaturation and consequent  $\alpha$ -helix formation of proteins.

On the other hand, Luo and Baldwin<sup>14</sup> analyzed helix formation of the alanine-based short peptides in TFE/water mixtures on the basis of the Lifson–Loig helix–coil transition theory.<sup>15</sup> They also measured the change in strength of hydrogen

(8) Gerlsma, S. Y.; Stuur, E. R. *Int. J. Peptide Protein Res.* **1972**, *4*, 377–383.

(9) Tanford, C. *Adv. Protein Chem.* **1968**, *23*, 121–217.

(10) Thomas, P. D.; Dill, K. A. *Protein Sci.* **1993**, *2*, 2050–2065.

(11) Liu, Y.; Bolen, D. W. *Biochemistry* **1995**, *34*, 12884–12891.

(12) Uversky, V. N.; Narizhneva, N. V.; Kirschstein, S. O.; Winter, S.; Löber, G. *Folding & Design* **1997**, *2*, 163–172.

(13) Shiraki, K.; Nishikawa, K.; Goto, Y. *J. Mol. Biol.* **1995**, *235*, 180–194.

(14) Luo, P.; Baldwin, R. L. *Biochemistry* **1997**, *36*, 8413–8421.

bonds in a model compound, salicylic acid, in TFE/water mixtures. They showed that the curve of hydrogen bond strength versus increasing TFE concentration matches, both in shape and magnitude, the increase in average helix propensity in TFE/water mixtures, and therefore proposed that hydrogen bond strengthening is responsible for the effects of TFE on helix formation by short peptides.

More recently, the effects of TFE on the kinetics of protein folding have been analyzed extensively.<sup>16–18</sup> TFE at low concentrations often accelerate the folding rate. Because TFE has a tendency to stabilize the helical conformation, TFE effects on the folding kinetics may be related to the specific structures of the transition and intermediate states which are stabilized in the presence of TFE.<sup>18</sup> Alternatively, the kinetic effects can be interpreted in a nonspecific manner on the basis of the thermodynamic effects of TFE.<sup>17,19</sup> TFE destabilizes the extended unfolded state with exposed amide groups, but not the compact transition or native states. Under this situation, only the folding rate would be accelerated in TFE.

We<sup>13</sup> first used TFE for demonstrating the intrinsic high helical potential of bovine  $\beta$ -lactoglobulin, a major component of cow's milk with a molecular mass of 18400 (162 amino acid residues). It is a predominantly  $\beta$ -sheet protein consisting of a  $\beta$ -barrel of eight antiparallel  $\beta$ -strands shaped into a flattened cone and one major  $\alpha$ -helix.<sup>20,21</sup> We showed that addition of TFE to  $\beta$ -lactoglobulin cooperatively transforms the native  $\beta$ -sheet structure to an  $\alpha$ -helical structure.<sup>13,22</sup> The helical propensity in the presence of TFE is much higher than those of other  $\beta$ -sheet proteins. This suggests that, although  $\beta$ -lactoglobulin is a  $\beta$ -sheet protein, the local interactions determined by the residues located close to each other in the sequence favor the  $\alpha$ -helical structure. The high helical preferences exhibited by the secondary structure predictions are consistent with this view.<sup>23</sup> The transient accumulation of the helical intermediate during the kinetic refolding of  $\beta$ -lactoglobulin suggests that the high helical preference has kinetic significance, controlling the folding mechanism of this protein.<sup>24</sup>

In a series of studies on  $\beta$ -lactoglobulin with TFE, we have been interested in understanding the mechanism of why, among various alcohols, TFE exerts such marked effects on protein structure. Alcohol-induced denaturation of the native state involves two steps: denaturation of the native structure and induction of a helical structure. As a reaction model of the induction of helical structure, Hirota et al.<sup>5–7</sup> examined an

alcohol-induced helix formation of melittin, a 26-residue amphiphilic peptide from honeybee venom.<sup>25</sup> They compared the effects of various alcohols in inducing the helical structure in melittin and found that variation in these effects can be explained by the additive contribution of each constituent group of the alcohol.<sup>6</sup> The hydrocarbon (CH) group and any halogen substituents make a positive contribution, whereas the hydroxyl (OH) group contributes negatively to the effect. The effectiveness of various alcohols was quantified in terms of the helix propagation parameter based on the modified Lifson–Roig theory<sup>15</sup> or the  $m$  value of the two-state transition mechanism. Both of these values for various alcohols can be predicted by equations in which the additive contribution of each constituent group is assumed to be proportional to its solvent-accessible surface area. Our interpretation of these alcohol effects is consistent with a view that considers the importance of solvent polarity, since this is related to the structure of alcohol molecules. Nevertheless, the potency of TFE or HFIP to transform the structure of proteins is much higher than predicted, suggesting that other unknown factors play an important role in the effects of these fluorine-substituted alcohols.

In the present study, to clarify the factor largely responsible for the effects of TFE or HFIP, we examined the correlation of the alcohol-induced conformational transitions of melittin and  $\beta$ -lactoglobulin with  $\epsilon_r$ , hydrogen bond strength, and alcohol clustering using alcohol/water mixtures. The results indicated that alcohol cluster formation plays a critical role in altering the structure of proteins and peptides.

## Experimental Section

**Materials.** Bovine  $\beta$ -lactoglobulin, isomer A, and melittin were obtained from Sigma, and melittin was further purified by reverse-phase HPLC.<sup>6</sup> Methanol, ethanol, TFE, HFIP, salicylic acid (*o*-hydroxybenzoic acid), and *p*-hydroxybenzoic acid were purchased from Nacalai Tesque at the highest purity available.

**Relative Dielectric Constant.** The  $\epsilon_r$  values of alcohol/water mixtures were measured with a HP41491A impedance probe combined with a HP4149A impedance/gain-phase analyzer (Hewlett-Packard). The cell constant was about 2.5 pF and the electrode probe was of the throw-in type. The cell constant was determined accurately using several standard liquids. The temperature of the samples was kept at 20 °C by a circulating thermobath.

**Determination of  $pK_a$ .** The hydrogen bond strength in alcohol/water mixtures was estimated by  $pK_a$  measurement of *o*-hydroxy- and *p*-hydroxybenzoic acids.<sup>14</sup> The difference ( $\Delta pK_a$ ) between  $pK_a$  values for the COOH group in *o*-hydroxy- and *p*-hydroxybenzoic acids at an identical alcohol concentration provides a measure of the hydrogen bond strength formed in *o*-hydroxybenzoic acid. In this study, the effect of various alcohols on the hydrogen bond strength was evaluated in terms of  $\Delta \Delta pK_a (= \Delta pK_a^{al} - \Delta pK_a^0)$ . Here,  $\Delta pK_a^{al}$  and  $\Delta pK_a^0$  are the values of  $\Delta pK_a$  with and without alcohol, respectively. The  $pK_a$  values were determined by fitting the pH titration curves of *o*-hydroxy- and *p*-hydroxybenzoic acids in 100 mM NaCl in alcohol/water mixtures to the theoretical curves. The UV difference spectra of *o*-hydroxybenzoic and *p*-hydroxybenzoic acids in alcohol solutions were measured at 241 and 261 nm, respectively, with a U-3000 spectrophotometer (Hitachi). The pH measurements were made on a PHM83 pH meter (Radiometer). The pH meter and electrode were calibrated using standard pH buffers at three points: 2.00, 4.01, and 7.00, at 25 °C. The pH electrode was inserted into a test tube containing the sample solution, and the tube was placed in a thermostated water bath. The temperature was maintained at 25 °C. After adding concentrated HCl or NaOH solution, the sample was shaken until the pH value became stable, and the absorbance of the sample withdrawn was measured. The  $pK_a$  values were estimated by curve-fitting analysis using a nonlinear least-squares procedure employing the IGOR Pro data analysis program (WaveMetrics)

(15) (a) Scholtz, J. M.; Qian, H.; York, E. J.; Stewart, J. M.; Baldwin, R. L. *Biopolymers* **1991**, *31*, 1463–1470. (b) Rohl, C. A.; Chakrabarty, A.; Baldwin, R. L. *Protein Sci.* **1996**, *5*, 2623–2637.

(16) Zerovnik, E.; Virden, R.; Jerala, R.; Turk, V.; Waltho, J. P. *Proteins Struct. Funct. Genet.* **1998**, *32*, 296–303.

(17) Kentsis, A.; Sosnick, T. R. *Biochemistry* **1998**, *37*, 14613–14622.

(18) (a) Chiti, F.; Taddei, N.; Webster, P.; Hamada, D.; Fiaschi, T.; Ramponi, G.; Dobson, C. M. *Nature Struct. Biol.* **1999**, *6*, 380–387. (b) Ionescu, R. M.; Matthews, C. R. *Nature Struct. Biol.* **1999**, *6*, 304–307.

(19) Walger, R.; Lee, T. C.; Cammers-Goodwin, A. *J. Am. Chem. Soc.* **1998**, *120*, 5073–5079.

(20) (a) Sawyer, L. *Advanced dairy chemistry-1: Proteins*; Fox, P. F., Ed.; Elsevier Applied Science: London, 1992; pp 141–190. (b) Brownlow S.; Cabral, J. H. M.; Cooper, R.; Flower, D. R.; Yewdall, S. J.; Polikarpov, I.; North, A. C. T.; Sawyer, L. *Structure* **1997**, *5*, 481–495. (c) Qin, B. Y.; Bewley, M. C.; Creamer, L. K.; Baker, H. M.; Baker, E. N.; Jameson, G. B. *Biochemistry* **1998**, *37*, 14014–14023.

(21) Kuwata, K.; Hoshino, M.; Era, S.; Batt, C. A.; Goto, Y. *J. Mol. Biol.* **1998**, *283*, 731–739.

(22) Hamada, D.; Kuroda, Y.; Tanaka, T.; Goto, Y. *J. Mol. Biol.* **1995**, *254*, 737–746.

(23) (a) Nishikawa, K.; Noguchi, T. *Methods Enzymol.* **1991**, *202*, 21–24. (b) Kuroda, Y.; Hamada, D.; Tanaka, T.; Goto, Y. *Folding & Design* **1996**, *1*, 255–263.

(24) Hamada, D.; Segawa, S.; Goto, Y. *Nature Struct. Biol.* **1996**, *3*, 868–873.

(25) Haberman, H. *Science* **1972**, *177*, 314–322.

**Solution X-ray scattering.** Solution X-ray scattering data were collected on the solution scattering station (SAXES camera) installed at BL-10C, the Photon Factory, Tsukuba, Japan.<sup>26</sup> The experiments were performed under an approval of the program advisory committee (proposal No. 97G128). The sample-to-detector distance was about 90 cm. The instrument was calibrated using meridional diffraction of dried rabbit collagen. The sample cell was 50  $\mu\text{L}$  in volume with a 15- $\mu\text{m}$ -thick mica window, and a 1-mm path length. The thermostatically controlled cell holder was connected to a RTE-110 (Neslab) refrigerated bath circulator, and the temperature was maintained at 20  $^{\circ}\text{C}$ . The apparent  $R_g$  of HFIP clusters was estimated by the Guinier approximation,  $I(Q) = I(0) \exp(-R_g^2 Q^2/3)$ , where  $Q$  and  $I(0)$  are the momentum transfer and intensity at the zero scattering angle, respectively.<sup>27</sup>  $Q$  is defined as  $Q = 4\pi \sin \theta/\lambda$ , where  $2\theta$  and  $\lambda$  are the X-ray scattering angle and wavelength (1.488  $\text{\AA}$ ), respectively.

**CD Measurements.** CD measurements were done with a Jasco spectropolarimeter, Model J-720, at 20  $^{\circ}\text{C}$  with a 1-mm cell as described before,<sup>5,6</sup> and the results were expressed as the mean residue ellipticity. The spectra of  $\beta$ -lactoglobulin and melittin at a concentration of 0.1 mg/mL in 10 mM Na phosphate buffer (pH 6.0) at various concentrations of SDS were measured.

## Results

**Alcohol-Induced Transitions.** Figures 1a and 1b show the alcohol-induced conformational transitions of  $\beta$ -lactoglobulin and melittin, respectively, at pH 2.0 measured by the ellipticity at 222 nm, taken from Hirota et al.<sup>5,6</sup> The native structure of  $\beta$ -lactoglobulin is stable as a monomer even at pH 2.<sup>21</sup> Upon addition of alcohols, cooperative transition to a highly  $\alpha$ -helical conformation with a helical content of about 90% occurs. However, the effectiveness of alcohols varies markedly: the order among the four alcohols is HFIP > TFE > ethanol > methanol. Although the transitions are cooperative, the presence of an intermediate has been suggested.<sup>12,21</sup> In contrast, alcohols induce the folding transition of initially unfolded melittin at pH 2.0 to an  $\alpha$ -helical conformation with a helical content of about 60% (Figure 1b). The effectiveness of the alcohols again varies substantially and the order is the same as that for the native  $\beta$ -lactoglobulin.

**Relative Dielectric Constant.** The  $\epsilon_r$  values of alcohol/water mixtures were measured for ethanol, TFE, and HFIP (Table 1, Figure 2a). For comparison the reported values<sup>6,28</sup> for methanol and ethanol were also indicated. The dependencies on alcohol concentration for ethanol, and the  $\epsilon_r$  values for pure TFE and HFIP, were consistent with those reported. The  $\epsilon_r$  value decreased linearly with increasing alcohol concentration, and the extent of the decrease at the same alcohol concentration (v/v) followed the order methanol < ethanol = TFE < HFIP. It was noted that the  $\epsilon_r$  values at the same concentration were similar between ethanol and TFE.

The conformational transitions of  $\beta$ -lactoglobulin and melittin induced by the four alcohols were plotted against the  $\epsilon_r$  values of the respective alcohol/water mixtures (Figures 2b and 2c). If  $\epsilon_r$  is a critical scale for the conformational transition of  $\beta$ -lactoglobulin and melittin, we would expect agreement of the curves for the transition induced by various alcohols. However, as can be seen, there was significant disagreement between the transition curves. For both  $\beta$ -lactoglobulin and melittin, the transition curves for methanol and ethanol were close to each other. On the other hand, the transition curves for HFIP and TFE were relatively similar and more cooperative than those

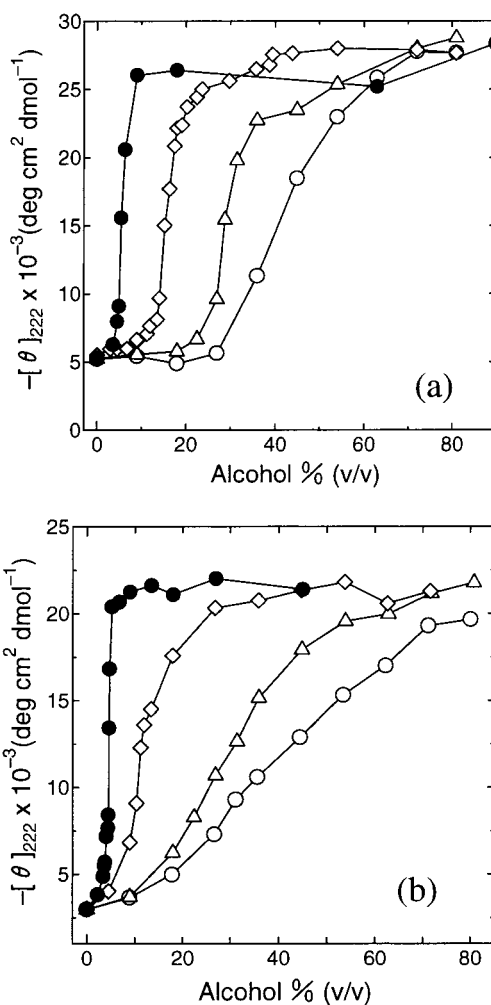


**Figure 1.** Alcohol-induced conformational transition of bovine  $\beta$ -lactoglobulin A (a) and melittin (b) measured by the ellipticity at 222 nm. Methanol (O), ethanol ( $\Delta$ ), TFE ( $\diamond$ ), and HFIP ( $\bullet$ ). The data are taken from Hirota et al.<sup>5,6</sup> with permission.

**Table 1.** Relative Dielectric Constant Values for HFIP, TFE, Ethanol, and Methanol at Various Concentrations at 20  $^{\circ}\text{C}$ <sup>a</sup>

alcohol % (v/v)	HFIP	TFE	ethanol	methanol
0	80.1	80.1	80.1(80.4)	80.4
1	78.3 $\pm$ 0.2			
2	77.0 $\pm$ 0.4			
2.5		78.8 $\pm$ 0.2		
3	76.7 $\pm$ 0.2			
4	76.0 $\pm$ 0.2			
5	75.6 $\pm$ 0.5	78.0 $\pm$ 0.1	78.9 $\pm$ 0.2 (78.1)	78.3
10	71.3 $\pm$ 0.2	75.5 $\pm$ 0.3	77.0 $\pm$ 0.4 (75.6)	76.5
15	68.1 $\pm$ 0.3	72.7 $\pm$ 0.2	74.7 $\pm$ 0.3 (73.3)	74.9
20	65.6 $\pm$ 0.2	70.5 $\pm$ 0.2	71.0 $\pm$ 0.4 (70.8)	73.4
25	63.1 $\pm$ 0.2	67.9 $\pm$ 0.2	68.2 $\pm$ 0.3 (68.2)	71.6
30	60.2 $\pm$ 0.2	64.8 $\pm$ 0.3	65.3 $\pm$ 0.2 (65.4)	68.8
35	56.9 $\pm$ 0.3	61.5 $\pm$ 0.2	62.1 $\pm$ 0.2 (62.7)	66.2
40	53.4 $\pm$ 0.2	57.5 $\pm$ 0.1	58.9 $\pm$ 0.6 (59.8)	63.8
45	51.3 $\pm$ 0.2	55.4 $\pm$ 0.2	55.0 $\pm$ 0.2 (56.9)	61.6
50	49.0 $\pm$ 0.3	53.0 $\pm$ 0.4	52.4 $\pm$ 0.5 (53.9)	59.2
60	43.2 $\pm$ 0.5	46.7 $\pm$ 0.3	45.1 $\pm$ 0.2 (47.9)	54.4
70	37.4 $\pm$ 0.2	41.5 $\pm$ 0.2	38.9 $\pm$ 0.5 (41.9)	49.1
80	30.3 $\pm$ 0.3	35.3 $\pm$ 0.3	35.0 $\pm$ 0.4 (35.9)	43.5
90	24.3 $\pm$ 0.4	31.5 $\pm$ 0.2	29.9 $\pm$ 0.3 (30.1)	37.9
100	17.8 $\pm$ 0.1	27.1 $\pm$ 0.1	25.8 $\pm$ 0.1 (25.0)	32.4

<sup>a</sup> The values for ethanol in parentheses and those for methanol are estimated on the basis of the values reported by Åkerlöf.<sup>28</sup>

of methanol and ethanol. Uversky et al.<sup>12</sup> reported that the transition curves for  $\beta$ -lactoglobulin induced by methanol, ethanol, 2-propanol, and dimethylformamide agreed very well

(26) Ueki, T.; Hiragi, Y.; Kataoka, M.; Inoko, Y.; Amemiya, Y.; Izumi, Y.; Tagawa, H.; Muroga, Y. *Biophys. Chem.* **1985**, *23*, 115–124.

(27) (a) Guinier, A.; Fournet, B. *Small-Angle Scattering of X-rays*; John Wiley: New York, 1955. (b) Kataoka, M.; Goto, Y. *Folding & Design* **1996**, *1*, R107–R114.

(28) Åkerlöf, G. *J. Am. Chem. Soc.* **1932**, *54*, 4125–4139.

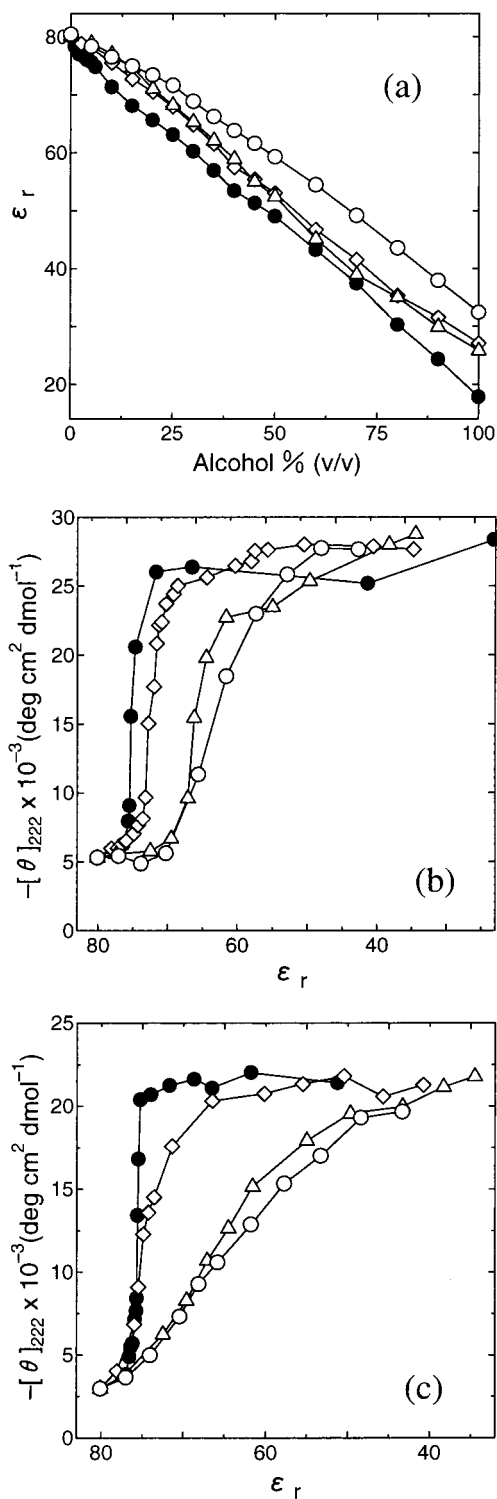


**Figure 2.** Conformational transitions of  $\beta$ -lactoglobulin and melittin scaled by the relative dielectric constant of alcohol/water mixtures. (a)  $\epsilon_r$  of alcohol/water mixtures. The ellipticity values for  $\beta$ -lactoglobulin (b) and melittin (c) plotted against  $\epsilon_r$ . Methanol (O), ethanol ( $\Delta$ ), TFE ( $\diamond$ ) and HFIP ( $\bullet$ ).

if they were plotted against solvent  $\epsilon_r$ . These findings indicate that, although  $\epsilon_r$  might be a critical factor for alcohols with relatively low potential, it cannot explain the marked effects of TFE and HFIP.

**Hydrogen Bond Strength.** We measured the increase in hydrogen bond strength in the alcohol/water mixtures using salicylic acid following the method of Luo and Baldwin.<sup>14</sup> If their explanation is valid for HFIP, an alcohol more effective

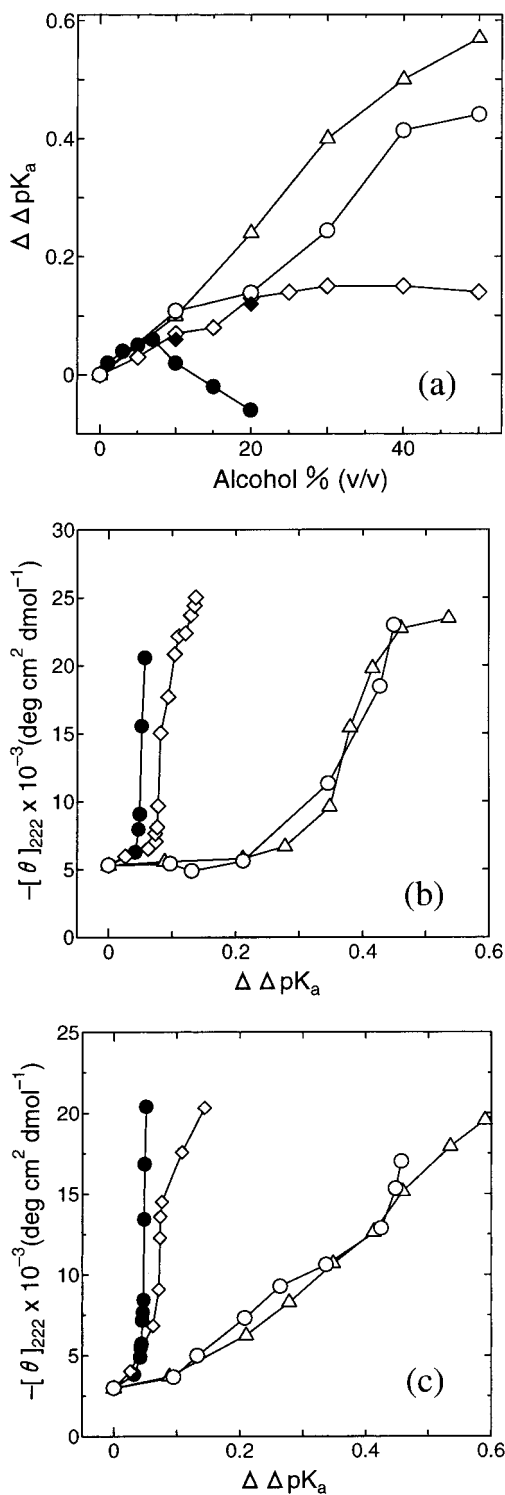


**Figure 3.** Conformational transitions of  $\beta$ -lactoglobulin and melittin scaled by the strength of the hydrogen bond. (a)  $\Delta\Delta pK_a$  of *o*-hydroxy- and *p*-hydroxybenzoic acids in the presence of various alcohol/water mixtures. The ellipticity values of  $\beta$ -lactoglobulin (b) and melittin (c) plotted against  $\Delta\Delta pK_a$  of *o*-hydroxy- and *p*-hydroxybenzoic acids. Methanol (O), ethanol ( $\Delta$ ), TFE ( $\blacklozenge$ ,  $\diamond$ ), and HFIP ( $\bullet$ ). Open diamonds for TFE in panel a were taken from Luo and Baldwin.<sup>14</sup>

than TFE, we would expect a significant increase of hydrogen bond strength in HFIP in comparison with TFE. The values of  $\Delta\Delta pK_a$ , a measure of hydrogen bond strength, were estimated for methanol, ethanol, TFE, and HFIP at various alcohol concentrations (Figure 3a). The values for TFE were consistent with those reported by Luo and Baldwin.<sup>14</sup> At concentrations below 10% (v/v), the  $\Delta\Delta pK_a$  value of HFIP was slightly higher

than that of TFE. However, it decreased above 10%, although the reason for this was unclear. On the other hand, the values for methanol and ethanol were slightly higher than that of TFE below 10%, and continued to increase above 20%, where  $\Delta\Delta pK_a$  of TFE showed saturation. The estimation of  $\Delta\Delta pK_a$  depends on the subtle difference between the large changes in  $pK_a$  of *o*- and *p*-hydroxybenzoic acids induced by the addition of alcohols. In addition, as we carried out no pH correction for the apparent pH values in the presence of high concentrations of alcohols, we cannot exclude the possibility that the  $\Delta\Delta pK_a$  values, indicated in Figures 3a, include some errors, particularly at high concentrations above 10% (v/v).

The CD transitions of  $\beta$ -lactoglobulin and melittin shown in Figure 1 were replotted against the  $\Delta\Delta pK_a$  values (Figures 3b and 3c), and again we were unable to obtain agreement among the four transition curves. However, for both  $\beta$ -lactoglobulin and melittin, there was some agreement between the transition curves for TFE and HFIP and between those for methanol and ethanol. This propensity was similar to that observed for the plot of conformational transitions against  $\epsilon_r$  (Figure 2).

The explanation for the effects of alcohol in terms of bulk hydrophobic effects (i.e.  $\Delta G_h$ ) is similar to that of low polarity or decreased  $\epsilon_r$ .<sup>6,10,11</sup> Because a nonpolar environment strengthens the electrostatic interactions including hydrogen bonds, the hydrogen bonds in alcohols should be strengthened in a manner similar to  $\epsilon_r$ , even if the two are not the same. It was evident that neither of these factors could explain the marked effects of HFIP or TFE, whereas the effects of alcohols with low potential can be explained by the bulk properties of the alcohol/water mixtures. Thus, although the low solvent polarity is a fundamental factor common to all the alcohol species, there appears to be an additional factor enhancing the effects of TFE and HFIP.

**Aggregation of Alcohol Molecules.** Kuprin et al.<sup>29</sup> studied alcohol/water mixtures, including HFIP and TFE, by small-angle X-ray scattering and suggested that HFIP has a high tendency to form micelle-like clusters with a maximum at about 30% (v/v). It is notable that HFIP and TFE are completely miscible with water at any concentration. Other alcohols, i.e., 2,2,3,3-tetrafluoro-1-propanol, *tert*-butyl alcohol, or 2-propanol, also form micelle-like clusters, but to a much lesser extent.<sup>29</sup> In aqueous solutions of water-miscible alcohols at intermediate concentrations, alcohol molecules associate so as to minimize their contact with water. This results in the formation of micelle-like clusters with the hydrophobic groups inside, although no macroscopic phase separation takes place.<sup>30</sup> At higher concentrations of alcohols, the micelle-like clusters disappear, resulting in a homogeneous solution. We suggested that this characteristic of HFIP and TFE may be the reason for their unexpectedly high potential for stabilizing  $\alpha$ -helices and also destabilizing the native structure of proteins.<sup>6,7</sup>

We measured small-angle X-ray scattering of aqueous mixtures of HFIP, TFE, ethanol, and methanol, and plotted the average scattering intensity in the interval  $0.1 \text{ \AA}^{-1} < Q < 0.3 \text{ \AA}^{-1}$  against alcohol concentration (Figure 4a). For HFIP, as was reported by Kuprin et al.,<sup>29</sup> we observed strong scattering at intermediate alcohol concentrations, with a maximum at around 30% (v/v). A similar maximum with a weak intensity was also

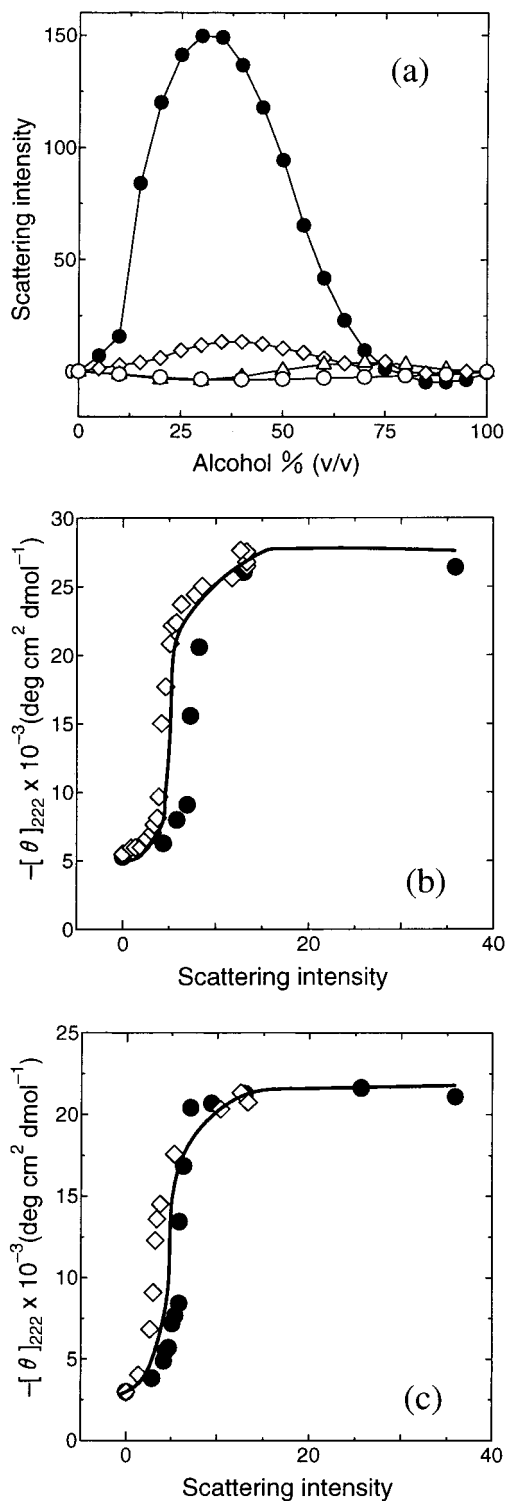


**Figure 4.** Conformational transitions of  $\beta$ -lactoglobulin and melittin scaled by the small-angle X-ray scattering intensity. (a) X-ray scattering intensity of various alcohol/water mixtures. The average scattering intensity in the interval  $0.1 \text{ \AA}^{-1} < Q < 0.3 \text{ \AA}^{-1}$  was obtained. Then the excess scattering intensity was plotted, assuming a linear baseline between water and 100% alcohol. The scatterings obtained from 100% alcohols are not zero, even though they are small. The ellipticity values of  $\beta$ -lactoglobulin (b) and melittin (c) plotted against the excess X-ray scattering intensity of TFE and HFIP. Methanol ( $\circ$ ), ethanol ( $\Delta$ ), TFE ( $\diamond$ ), and HFIP ( $\bullet$ ).

(29) Kuprin, S.; Grauslund, A.; Ehrenberg, A.; Koch, M. H. J. *Biochem. Biophys. Res. Commun.* **1995**, *217*, 1151–1156.

(30) (a) Franks, F.; Desnoyers, J. E. *Water Science Review 1*; Franks, F., Ed.; Cambridge University Press: London, 1986; pp 171–231. (b) Mizutani, Y.; Kamogawa, K.; Kitagawa, T.; Shimizu, A.; Taniguchi, Y.; Nakanishi, K. *J. Phys. Chem.* **1991**, *95*, 1790–1794. (c) Koga, Y. *J. Phys. Chem.* **1996**, *100*, 5172–5181.

observed for TFE. However, the scattering of ethanol and methanol was negligible, without a maximum at intermediate concentrations. Figures 4b and 4c show the transition curves

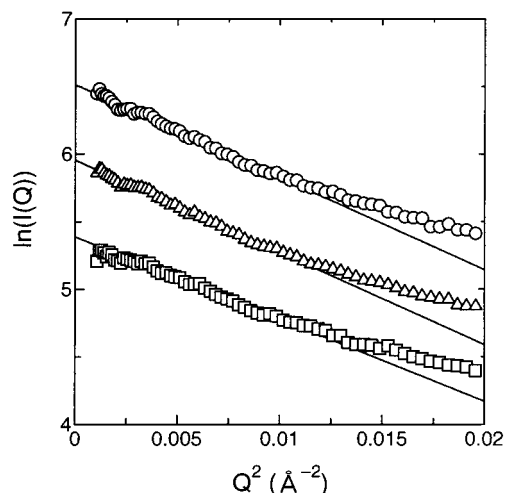


**Figure 5.** Guinier plots of HFIP/water mixtures at HFIP concentrations of 25% (○), 30% (△), and 35% (v/v) (□). The apparent  $R_g$  values are estimated to be 14.3 Å for 25%, 14.3 Å for 30%, and 13.5 Å for 35% HFIP assuming the indicated linearity. For clarity, the values of each plot are shifted on the  $\ln I$  axis by 1.

of  $\beta$ -lactoglobulin and melittin, respectively, plotted against the X-ray scattering intensity of TFE/water or HFIP/water mixtures at the same concentration. We did not use the scattering data for the ethanol and methanol solutions because the scattering from these solutions was very small. The significant scattering observed for TFE or HFIP solutions and the agreement of the transition curves plotted against the scattering intensity confirmed that clustering of alcohols is a critical factor responsible for the marked effects of HFIP and TFE.

We analyzed the apparent size of the HFIP clusters using the Guinier plot (Figure 5).<sup>27</sup> For a solution of homogeneous particles such as proteins, the Guinier plot is linear in the small angle region within  $R_g Q \leq 1.3$ , and the slope provides the radius of gyration,  $R_g$ . The Guinier plots at around 30% (v/v) HFIP were fairly linear and parallel to each other, suggesting that the size of the HFIP clusters is relatively constant, irrespective of HFIP concentration. The apparent values were 14.3, 14.3, and 13.5 Å at 25, 30, and 35% (v/v) HFIP, respectively. These values are comparable, probably by chance, to the  $R_g$  value (16 Å) for native monomeric  $\beta$ -lactoglobulin (data unpublished). The  $R_g$  values below 25% and above 35% were difficult to estimate because of low scattering intensity and, therefore, the exact dependency of  $R_g$  upon HFIP concentration was not determined.

**SDS-Induced Transitions.** As an example of the micelle-induced conformational transition, the effects of sodium dodecyl sulfate (SDS), one of the most widely used amphiphilic detergents,<sup>31</sup> on  $\beta$ -lactoglobulin and melittin were examined by CD in 10 mM Na phosphate (ionic strength = 0.01) at pH 6.0 (Figure 6). As was the case for alcohols, SDS cooperatively transformed  $\beta$ -lactoglobulin to an  $\alpha$ -helical structure, although the ellipticity of the helical state after the transition was evidently less than that induced by HFIP at the same pH. The spectra at various SDS concentrations suggested that a two-state approximation holds. The plots of the ellipticity at 222 nm against the SDS concentration showed a cooperative transition curve with a midpoint at 1.5 mM. It is noted that cmc of SDS, which depends on ionic strength, is about 5, 3, and 1.5 mM at ionic strengths of 0.01, 0.02, and 0.1, respectively, at 25 °C.<sup>31</sup>

Although melittin in the presence of high concentrations of SDS assumed a helical structure very similar to that in alcohols,

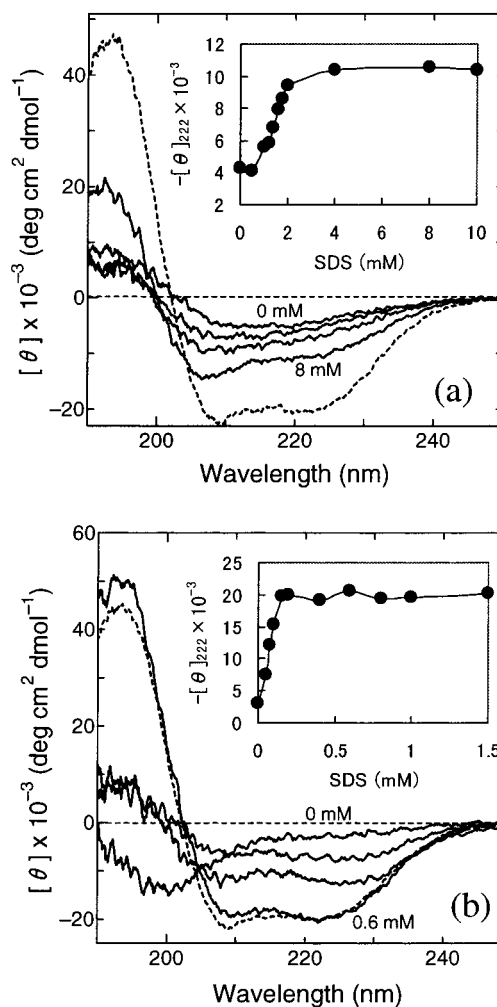


**Figure 6.** Far-UV CD spectra of bovine  $\beta$ -lactoglobulin A (a) and melittin (b) in the presence of various concentrations of SDS at pH 6.0 and 20 °C. SDS concentrations of the spectra from lowest to highest intensity at 222 nm: (a) 0, 1, 1.4, and 8 mM; (b) 0, 0.05, 0.075, and 0.6 mM. The dotted lines indicate the spectra in 20% (v/v) HFIP. Inset: Transition curves measured by the ellipticity at 222 nm.

it exhibited a marked propensity to aggregate at the SDS concentrations below 0.3 mM. It is noted that melittin is highly soluble in the absence of SDS because of the abundant positive charges. The CD spectra in the presence of SDS at lower than 0.3 mM were unstable, decreasing the CD intensity with time, and those shown in Figure 6b were obtained immediately after the preparation of solution. The SDS-dependent transition curve for melittin was constructed by plotting the ellipticity at 222 nm, which was extrapolated to time zero when the time-dependent change in signal occurred. The transition curve thus obtained was highly cooperative with a midpoint at 0.2 mM SDS (Figure 6b).

## Discussion

Alcohol molecules consist of hydrophobic hydrocarbon and halogen groups and hydrophilic OH groups. Hirota et al.<sup>5-7</sup> indicated that the effects of alcohol can be approximated by the additive contribution of each group, where hydrocarbon and halogen groups contribute positively and OH groups contribute negatively. However, they also indicated that such a mechanism cannot explain the marked effects of TFE and HFIP and suggested that the contribution of an additional factor, aggregation or clustering of alcohol molecules through hydrophobic

(31) Tanford, C. *The hydrophobic effects*. 2nd ed.; John Wiley & Sons: New York, 1980.

interactions, has to be considered. The present results show that the clustering of TFE and HFIP molecules is highly correlated with  $\alpha$ -helix formation in melittin and the denaturation of  $\beta$ -lactoglobulin. The clusters of hydrophobic alcohol molecules provide a local nonpolar environment, where hydrophobic interactions are weakened and hydrogen bonds are strengthened.

Clustering of alcohol molecules has been indicated even for ethanol/water mixtures. Yamaguchi and co-workers<sup>32</sup> examined the structure of clusters in ethanol/water mixtures using several physicochemical methods including mass spectrometry and X-ray diffraction. They observed a series of hydrated ethanol polymers, whose structure and amount were dependent on ethanol concentration. Maximal accumulation of ethanol clusters with a polymerization number of 10 to 16 was observed at an ethanol molar fraction of 0.15 (36% (v/v)) to 0.18 (42% (v/v)). With an increase in the ethanol molar fraction above 0.2 (45% (v/v)), the amount of clustering decreased, indicating that, whereas the clusters are stabilized by hydrophobic interactions, hydration is essential for maintaining them.

Alcohol clusters should be formed by other alcohol species,<sup>30</sup> but the exact structures and properties will vary depending on alcohol species. Because the major force responsible for the clustering is hydrophobic interaction, an alcohol with a bulky hydrophobic group may tend to form larger clusters than one with a less bulky group. Although, among the various halogen atoms, the contribution of the F atom to the effects of alcohol is minimal,<sup>5–7</sup> the presence of multiple F atoms, as seen for TFE or HFIP, increases the effect markedly by promoting cluster formation cooperatively. At high concentrations of TFE or HFIP, the alcohol clusters are disrupted because water molecules, which are necessary for separating and therefore stabilizing the clusters, disappear.<sup>32</sup> Thus it is likely that hydrophobic groups of proteins or peptides take part in the clustering of alcohol molecules through protein–alcohol hydrophobic interactions.<sup>6</sup>

An analogy of the marked effects of alcohol through cluster formation is the interaction of proteins with SDS, one of the most widely used amphiphilic detergents. We can assume that HFIP is similar to SDS in that both consist of hydrophobic and hydrophilic groups and can form clusters through hydrophobic interactions. SDS micelles can denature the native structure of proteins and induce the  $\alpha$ -helical structure, as well as inducing the  $\alpha$ -helical structure in short peptides.<sup>33</sup> Indeed, SDS-dependent conformational transitions of  $\beta$ -lactoglobulin and melittin (Figure 6) resemble those induced by alcohols (Figure 1).

Monomeric SDS can interact with proteins and peptides. However, the interaction between monomeric SDS and peptides or proteins would not be extensive. Stabilization of the  $\beta$ -sheet conformation in the presence of SDS monomers below cmc has been reported for some peptides.<sup>33</sup> The aggregation of melittin at low concentrations of SDS observed here may be caused through such weak peptide–SDS interactions which cannot bury the hydrophobic groups of peptide and SDS, resulting in the formation of peptide aggregates. Once SDS forms micelles, the interaction becomes stronger because micelles provide extensive sites of interaction, i.e., they increase the effective concentration of the interacting sites. This results in protein denaturation and the formation of extended and persistent  $\alpha$ -helical structures.

In the case of SDS, one micelle cluster includes about 100 monomers.<sup>31</sup> This corresponds to a molecular weight of 25000, which is compared with the apparent size of HFIP clusters at 30% (v/v) (i.e.,  $R_g = 14 \text{ \AA}$ ) estimated by small-angle X-ray scattering. In the case of  $\beta$ -lactoglobulin, however, the helical content in SDS is evidently less than that in HFIP. It is conceivable that the charge repulsion between the negatively charged SDS micelles and the negatively charged  $\beta$ -lactoglobulin at pH 6 suppresses the formation of helices. In the case of melittin, a basic peptide, the electrostatic interactions with the negatively charged SDS would promote the formation of helical structure as observed in alcohols.

While the effects of HFIP on proteins and peptides are resembling those of SDS, we anticipated that the micelle-like clusters of HFIP would be less homogeneous and less rigid. Therefore, it was surprising that the micelle-like clusters of HFIP, as measured using the Guinier plots, were relatively homogeneous with an average  $R_g$  value of about  $14 \text{ \AA}$  at around 30% (v/v) HFIP. With an increase in alcohol concentration, the HFIP clusters disappear because water molecules, which are important for separating the clusters,<sup>32</sup> disappear. Intriguingly, the present SAXS measurements suggest that the  $R_g$  is constant around 30% (v/v) HFIP, although we could not determine exactly its dependence on HFIP concentration (Figure 5).

Clusters of TFE or HFIP disappear at high alcohol concentrations, but the helical structures of  $\beta$ -lactoglobulin and melittin remain. This indicates that, under such conditions, the helical structures are stable even in the absence of alcohol clusters. This is not surprising because other alcohols such as methanol and ethanol can stabilize the helical structure even in the absence of extensive alcohol clusters, as indicated by X-ray scattering measurements (Figure 4). At high alcohol concentrations, the low polarity of the bulk solvent or consequent strengthening of hydrogen bonds is probably enough to maintain the helical structures. This again confirms the fundamental role of solvent polarity in the alcohol effects on proteins and peptides.

## Conclusions

We previously compared the effects of various alcohols, including TFE and HFIP, on melittin and  $\beta$ -lactoglobulin.<sup>5–7</sup> Although the apparent conformational transitions differ markedly between melittin and  $\beta$ -lactoglobulin, the order of effectiveness of various alcohols is common. This supports the idea that the mechanisms of the effects of alcohol on native proteins and unfolded peptides are basically the same. In both cases, we believe that the decrease in protein hydrophobic interactions in alcohol/water mixtures is the most important factor. However, properties related to the bulk solvent, such as  $\epsilon_r$  or hydrogen bond strength, do not explain the marked effects of HFIP and TFE. In the present paper, we have indicated that aggregation or clustering of alcohol molecules is an important factor enhancing the effects of alcohol. Such clusters of bulky alcohol molecules provide a highly hydrophobic local environment, where, microscopically, polarity decreases and hydrogen bonds are strengthened. Upon binding to these hydrophobic clusters, proteins and peptides undergo a conformational transition, as they do upon binding to SDS micelles.

**Acknowledgment.** We thank Prof. Mikio Kataoka (Nara Institute of Science and Technology) and Nami Hirota Nakaoka (Osaka University) for discussion. This work was supported by the Ministry of Education, Science, Culture and Sports of Japan.

(32) (a) Nishi, N.; Takahashi, S.; Matsumoto, M.; Tanaka, A.; Muraya, K.; Takamuku, T.; Yamaguchi, T. *J. Phys. Chem.* **1995**, *99*, 462–468. (b) Matsumoto, M.; Nishi, N.; Furusawa, T.; Saita, M.; Takamuku, T.; Yamagami, M.; Yamaguchi, T. *Bull. Chem. Soc. Jpn.* **1995**, *68*, 1775–1783.

(33) Zhong, L.; Johnson, Jr. W. C. *Proc. Natl. Acad. Sci. U.S.A.* **1992**, *89*, 4462–4465.